



EXPERIMENTAL STUDY OF HEAT TRANSFER AUGMENTATION USING AIR BUBBLE INJECTION AND (Al₂O₃ /WATER) NANOFLUID FLOW IN DOUBLE PIPE HEAT EXCHANGERS

Dhirgham A. Alkhafaji¹
d.alkhafagi@yahoo.com

Hameed K. Hamzah²
Hameedkadhemi1977@gmail.com

Haider S. Hadi³
haiderhaker1985629@gmail.com

^{1,2} University of Babylon-College of engineering-Department of Mechanical engineering

³ Ministry of Interior

ABSTRACT

In the present work, an experimental study on how to increase the heat transfer coefficient (HTC) in double pipe heat exchanger (DPHE) use of a variety of Al₂O₃ Nano-dispersion concentrations mixed in water as base fluid with air bubble injection for counter flow arrangement under turbulent flow conditions with (Re) Reynold number range from (6000 to 45000) . The thermal performance of (DPHE) has been enhanced with the use of two techniques. The first, is represented by adding nanoparticles to hot water (inner pipe) raising the (HTC) inside the inner tube. Increase the volume concentration cause increase in the viscosity of the nanofluid leading to increase in friction factor .Secondly is represented by Air bubble injection in outer pipe with cold water to enhance the (HTC). The mobility of air bubbles inside the water from down to up by the force of the buoyancy, and the movement of these air bubbles results in significant mixture and turbulence within the water. The variations of number of thermal units (NTU), exergy loss, dimensionless exergy and (Nu) are evaluated. The investigated parameters were cold water volume flow rates (8, 10, 12 and 14) l/min, flow in outer tube. Also, three different volume flow rates of air (12, 16 and 20) l/min mixed with water in outer tube. The volume flow rates of hot water remains constant at (8 l/min) flow in inner pipe with three volumetric concentrations of given nanofluid. The results showed that the air bubble injection throughout the tube gave maximum enhancement in heat transfer characteristics followed by the no air bubble injection. Since the enhancement in heat transfer characteristics varies linearly with the volumetric concentration of Nanofluids, Nanofluids with 0.3% of Al₂O₃ nanoparticles gave more enhancements in (HTC) than the case without nanofluid. The Nusselt number increased about (8% - 45%).

Keywords: Injection of Air bubble, Nanofluids, (DPHE), (HTC), Al₂O₃ Nano-dispersion.

دراسة تجريبية لزيادة نقل الحرارة باستخدام حقن الفقاعات الهوائية وتدفق النانوفلويد (Al₂O₃ / WATER) في مبادلات حرارة مزدوجة الأنابيب

حيدر شاكر هادي

حميد كاظم حمزة

ضرغام عبد الحسين عبد الحسن

الخلاصة

في هذا العمل، اجريت دراسة عملية لتحسين معدل انتقال الحرارة مبادل حراري مزدوج الانبوب (DPHE) مع حقن فقاعات الهوائية في جانب الانبوب الخارجي و جزيئات اوكسيد الالمنيوم النانوية ثم تعليقها في ماء مقطر بتركيز حجمية

مختلفة تحت ظرف جريان اضطرابي لمدى من عدد رينولد (Re) يتراوح بين (6000 to 45000). تم تحسين الأداء الحراري لـ (DPHE) باستخدام تقنيتين. الأولى، تتمثل في إضافة الجسيمات النانوية إلى الماء الساخن (الأنبوب الداخلي) مما يرفع (HTC) داخل الأنبوب الداخلي. إن زيادة تركيز الحجمي يسبب زيادة في لزوجة الموائع النانوية مما يؤدي إلى زيادة عامل الاحتكاك وبالتالي زيادة في انتقال الحرارة. الثانية عن طريق حقن فقاعة الهواء في الأنابيب الخارجية مع الماء البارد لتعزيز (HTC). تنقل فقاعات الهواء داخل الماء من أسفل إلى أعلى بواسطة قوة الطفو، وحركة فقاعات الهواء هذه تؤدي إلى خلط كبير واضطراب داخل الماء. تم حساب الاختلاف في (Nu, exergy loss and NTU). بواقع أربعة معدلات جريان حجمية مختلفة للمائع خلال الأنبوب الخارجي (8, 10, 12 and 14 l/min) وأيضا ثلاث معدلات جريان حجمية للهواء (12, 16 and 20) l/min تخلط مع الماء في جانب الأنبوب الخارجي. مع بقاء معدل الجريان الحجمي للأنبوب الداخلي عند (8 l/min) مع ثلاثة تركيزات حجمية من السائل النانوي المحدد في هذا العمل. أظهرت النتائج أن حقن فقاعة الهواء في جميع أنحاء الأنبوب أعطى أقصى قدر من التعزيز في خصائص نقل الحرارة متنوعة بحقن عدم وجود فقاعة هواء. وكذلك إن التحسن في خصائص نقل الحرارة تختلف بشكل خطي مع التركيز الحجمي للنانوفلود، أعطت النانوفلويديات مع (0.3%) من الجسيمات النانوية Al_2O_3 تحسينات في (HTC) أكثر من الحالة بدون الجسيمات النانوية. وإن الزاد في عدد نسلت (Nu) حوالي (45% - 8%).

NOMENCLATURE

Latin Symbols

	Description
A	area (m^2)
C_p	specific heat ($J/kg \cdot ^\circ C$)
D	diameter (m)
DPHE	double pipe heat exchanger
f	friction factor
h	heat transfer coefficient ($W/m^2 \cdot ^\circ C$)
HE	heat exchanger
HTC	heat transfer coefficient
K	thermal conductivity ($W/m \cdot ^\circ C$)
LMTD	logarithmic mean temperature deference
Nu	Nusselt Number
NTU	number of thermal units
P	Pressure (N/m^2)
Pr	Prandtl number
Q	heat flow (W)
Re	Remolds number
T	temperature (k or $^\circ C$)
U	Overall heat transfer coefficient ($W/m^2 \cdot ^\circ C$)
\dot{V}	volume flow rate (l/min)
V	velocity (m/sec)

Greek letters

	Description
μ	dynamic viscosity ($kg/m \cdot sec$)
ρ	density (kg/m^3)
Δp	pressure drop (N/m^2)
ϕ	volume concentration

Subscripts

	Description
A	air
Bf	base fluid
C	cold
CF	counter flow
E	environment
F	liquid phases
H	hot
I	inner

In	inlet
Nf	Nanofluid
o	outer
Out	outlet
p	solid particle
PF	parallel flow
s	surface

INTRODUCTION

In today's era, the limited or confined resources of energy are vanishing day by day as the humans are using them at an unimaginable alarming rate. If the humans continue to use these energy resources in such a rapid rate then the day is not so far when our future generation will starve for these energy resources. This overexploitation of these energy resources has forced the engineers or researchers to find some advanced or new techniques to enhance the thermal performance characteristics of (HE), so that the ever growing demand for these energy resources can be fulfilled to the most possible extent Kahrom et al. (2010). Kitagawa et al. (2010) the (HTC) enhancement was experimentally investigated related to hydrogen bubble injection in turbulent natural convection. They registered improvements of 1.2-1.3 times in the turbulent natural convection. They also found that the enhancement in (HTC) due to air bubble injection decreases as the mean bubble diameter increase. Dizaji and Jafarmadar (2014) studied the role of air bubble injection on (HTC), NTU (number of thermal units) and heat effectiveness in a (DPHE). The air bubbles were pumped through the horizontal (DPHE) (promising technique) at different conditions increases the (HTC) of (HE). The result showed that the quantity of Nusselt number (Nu) rise about (6% - 35%) depending Reynolds number (Re) and injection of air bubble condition and heat effectiveness around 10%- 40%. The maximum heat effectiveness was achieved when the pumped air bubbles were into the outer tube. Dizaji et al. (2015) Performed attempts to raise the NTU ,exergy loss and efficiency in the perpendicular shell and the coiled tube heat exchanger by pumping air bubble into the shell side. Indeed, the injection of air bubbles and the motion of bubbles due to the force of buoyancy can improve the exergy loss and the NTU by mixing the thermal boundary layer and rising the turbulence of the fluid flow. In this paper using a special technique with new conditions of air bubbles were pumping through the shell of (HE). Nandan and Singh (2016) investigated the pumping of air bubble at various regions influences on efficiency OF Shell and Tube (HE). The experiment was conducted with base fluid (distilled water) with and without pumping of air bubbles. The effect on (HTC) and (Nu) has also been calculated at different (Re) rates. It has been found that in comparison to simple distilled water (cooling fluid,) distilled water with air bubble injection indicates further heat transfer improvement. The consequence appeared that (Nu) raised by 30%-45 per cent with the pumping of air bubbles into the tube segment. A rise of 25-40 per cent in the (HTC) was found with same condition. Heyhat et al. (2018) experimentally studied the effect of the injection of air bubbles as an active thermal efficiency (DPHE) process. Air bubbles are pumped into the annulus side by means of a number of injectors. Experimental results are obtained with various volume flow rates for inner pipe and outer pipe. The study shows that the (U) was increased by 10.3 per cent to 49.5 per cent by air bubble pumping.

Jaafar Albadr et al. (2013) reported an experimental study on the forced convective heat transfer and flow characteristics of a Nanofluid contain water and various volume concentrations of Al₂O₃ Nanofluid (0.3–2) %. Under turbulent and counter flow conditions they are moving in a horizontal shell and tube (HE). Results show that the convective heat transfer coefficient of Nanofluid at the same mass flow rate and at the same inlet temperature was slightly greater than that of the base liquid. The Nanofluid (HTC) raised with a rise in the

mass flow rate and rise by an increase in the Al₂O₃ Nanofluid volume concentration, Nevertheless, rising the volume concentration led to a rise in the Nanofluid viscosity resulting in an increase in the friction factor. Kumar et al. (2016)] experimentally estimated the effectiveness and overall heat transfer coefficient (U) of Fe₃O₄/water Nanofluids flow in a (DPHE) with return bend with turbulent flow rule. Experiments in particle volume concentrations ranged from 0.005 per cent to 0.06 per cent and in the (Re) ranged from 4000 to 30000. The improvement of (Nu) is around (15.6% at 0.06% volume concentration) comparing with water (base fluid). At a (Re) of 28984 and 0.06% volume concentration, the (U) for outer pipe is improved about 3.44% when inner pipe is improved about 3.26% and the heat effectiveness is improved about.008-times compared to base fluid. Han et al. (2017) the influence of Al₂O₃-water Nanofluids on heat transfer improvement within the (DPHE) at varying inlet temperature was studied experimentally. Al₂O₃ Nanoparticles with a concentration of 0.25% and 0.5% by volume were used at various inlet temperatures with (Re) varying between (20000 to 60000).The findings of this study indicate that the heat transfer rises with a rise in the concentration of Nanoparticles and temperature. Significant enhancement over water has been shown in a cumulative (Nu) rise of up to about 24.5 per cent at an inlet temperature of 50°C. Rao et al. (2018) carried out an experimental investigation to estimate the (HTC) and (Nu) for Al₂O₃ of diameter 47 nm with water nanofluid in a Plain concentric (DPHE) in counter flow direction at different volume concentrations from 0.01%, 0.02% and 0.03%. Use Al₂O₃ Nanoparticles as the dispersed phase in water will greatly improve convective heat transfer in the transition flow, and the improvement rises with a rise in the (Re) and Al₂O₃ Nanoparticles volume concentration.

It should be noted that the difference in this study compared to the studies mentioned above is that it was combined the passive methods that do not need the direct application of external power, like the use of (U bend) and Al₂O₃ Nanoparticles. The active methods which require external power such as using of inject air bubbles along the heat exchanger.

EFFECTIVE THERMAL PROPERTIES OF NANOFLUID

The physical properties of nanofluid such as thermal conductivity (*K*), dynamic viscosity (*μ*), density (*ρ*), specific heat (*C_p*) and measure the following correlations at various volume fraction of Nanoparticles.[11, 12, 13, 14]. The effective density of nanofluids was evaluated using a relation established by { Lee et al. (1999) and Pak and Cho (1998) } for Nanofluids, as follows:

$$\rho_{nf} = (1 - \varphi)\rho_{bf} + \varphi\rho_p \quad (1)$$

The specific heat of the Al₂O₃ Nanofluids at various temperatures was calculated using the following equation Pak and Cho (1998) for all the concentrations of Nanofluids viewed in the present study.

$$Cp_{nf} = (1 - \varphi)Cp_p + \varphi Cp_{bf} \quad (2)$$

In accordance with Brinkman's Formula to use (1952), the effective nanofluid dynamic viscosity is expressed in the following terms:

$$\mu_{nf} = \frac{\mu_{bf}}{(1 - \varphi)^{2.5}} \quad (3)$$

The generic model of Maxwell Zan Wu et al. (2013) the active (*K*) thermal conductivity of liquid / solid Nano-disperse, low volume concentration spherical particle was calculated.

$$k_{nf} = \frac{(k_p + 2k_{bf}) + 2\varphi(k_p - k_{bf})}{(k_p + 2k_{bf}) - \varphi(k_p - k_{bf})} k_{bf} \quad (4)$$

Table (1) describes the thermos - physical properties of the base fluid and the nanoparticles

considered in this analysis, and the effective thermal properties of Al₂O₃ –water nanofluid for variable concentrations are presented in Table (2).

STEPS FOR PREPARING NANOFLUID

Nanofluid Preparation

Using ultrasonic cleaner bath was filled up to 75% of its volume by water to make sure no damage happened to the device as recommended by the instructions of the supplier, and then the basket was put inside the bath.

Ultrasonic cleaning is a method based on high-frequency sound waves which when travelled into a solution of nanofluid, created oscillating high and low pressure and consequently, caused the rapid formation and imploding bubbles radiate tremendous amounts of ultrasonic energy and shock waves that produced good mixing between nanoparticle and distilled water. (JTS-1018), single tank ultrasonic cleaner equipment system included replaceable transducer box and generator. The transducer box and generator can be both build-in or separate but worked together to operate ultrasonic cleaning process with transducer box immiscible mounted in a fluid tank, one side or both sides or bottom mounted inside the tank. The number and placement of transducers was selected to give maximum results in any parts of cleaning tank with any cleaning load. Specification of tank dimension and transducer boxes were custom made available. Ultrasonic cleaner contained a twelve transducers, drain valve and basket. The transducers converts the electrical signal with low frequency (50 Hz) to high frequency (40 kHz) mechanical vibrations. The valve is used to empty the tank and the basket to put the flask on it. The most important parameter was the sonication power with low power; it was very hard to get a colloidal solution. The ultrasonic cleaner is shown in figure (1) and its specifications are given in the Table (3).

Volume Concentrations

The amount of Al₂O₃ nanoparticles required for a particular volume concentration in the test sample of base fluid was calculated using the law of mixtures in terms of percentage of volume concentration, density of Al₂O₃ nanoparticles and density of water base fluid using the following relationships.

- a) Measuring quantity of powder required for each concentration by an electronic weighting machine as shown in figure (2).
- b) Adding the weight of nanoparticles to five liter of the distilled water in order to calculate the concentrations. According to the following equation reported by Fotukian and Esfahany (2010) as :

$$\varphi \% = \frac{(m_p / \rho_p)}{(m_p / \rho_p) + (m_{bf} / \rho_{bf})} \quad (5)$$

During the experiments, four volume concentrations were used as, 0.1%, 0.2%, and 0.3%. The mass of each concentration calculated from equation (5) as shown in table (4).

4. Taking the mixture of nanoparticles and the distilled water in the magnetic stirrer device to be mixed well for one hour to ensure the spreading of nanoparticles molecules and prevented aggregate of particles quickly.

5. Then the mixture sent to the ultrasonic cleaner bath device to be kept for (6 hours) to mix well and to ensure that the mixing took place perfectly checking the mixture in the oscilloscope.

6. Repeated the same procedure above for each concentration from 0.1%, 0.2% and 0.3%.

EXPERIMENTAL SET-UP

The schematic diagram of the experimental setup is shown in Figure 3, while Figure 4 shows the photographic representation of the experimental setup. The experimental setup consisting of test section, hot water loop, cold water loop and air injection system.

The Test Section State

The test section is a (DPHE) and it is constructed from concentric tubes with 5 m length. Copper tube with inner diameter of 20 mm and outer diameter of 22 mm was chosen as inner tube, and a Perspex tube with inner diameter 45 mm and outer diameter of 50 mm are chosen as outer tube of the test section. The hot fluid flows in the inner tube while the cooling fluid flows in the annulus.

The Hot Water Loop

The inner cycle where the working fluids (distilled water - Nanofluids based on Al_2O_3) with various volumetric concentrations (0 % (base fluid), 0.1 %, 0.2 % and 0.3 %) taken one after another. The flow consists of the hot fluid tank, heater of (1200 W) power, pump, flow meter and control valve, a bypass line to facilitate liquid flow rate control, a check valve and a piping system. The volume flow rate of hot water and the inlet temperature were maintained at about 8 l / min and 60°C respectively. The hot fluid tank has dimensions 1000 mm length , 530 mm diameter ,4 mm thickness represents length, diameter, and thickness respectively, with capacity 80 liter ,which was manufactured from Stainless steel metal.

The Cold Water Loop

A centrifugal pump from cold reservoir supplies the liquid. The liquid flow rate was measured before entering into the annulus side by a flow meter, the cold-water line contained a valve, a bypass line to facilitate liquid flow rate control and a check valve. After the heat exchanger (test section), the water flow goes to the radiator with cooling fan to remove the temperature obtained from the hot fluid then the water returns to dram tank with dimension of 0.5 m diameter and 1.2 m height, with capacity 150 liter, which was manufactured form a galvanized steel sheet vessel and used to storage the cold water. The flow rate of water change from 8 l/min to 14 l/min with a period of 2 l/min. The outer pipe water has been preserve at about 30 ° C.

The Air Flow Loop

Atmospheric air is used as the gas phase, it compressed and stored in a reservoir has capacity of 500 liter with 3 bars. The gas flow rate is adjusted by a volume flow rate controller, and then introduced to the test section (annulus side) with air by a two tube section 1.9 m length. Copper tube with inner diameter of 3 mm and outer diameter of 5 mm perforated diagonally 12 holes with diameter about 0.5 mm and the distance between the holes. A spring type check valve is used to prevent the inverse flow of the air. The air bubbles injection at different volume flowrate of air (12, 16 and 20 l/min).

The annulus tube is wound with insulation to reduce the heat loss from the test section to the environment. Four thermocouples K-type were used to measure the hot and cold fluid inlet and outlet temperatures. The thermocouples are linked at the inlet and outlet of the inner and outer pipes to recorder temperature (BTM-4208SD model) with SD card and for further measurements; the readings are reported in the computer. The test section was planned to in such a way possible to make it fully developed turbulent flow. Two rotameters control the volume flow rates of hot and cold liquid has range from (2 to 18 l/min). The circulating pump is centrifugal pump of type [Marquees - 220 V - 50 Hz - 0.37 kw], [Q max = 30 l/min, H max = 30 m] is used to circulate the hot fluid inside the test rig. Pressure sensor type (KELLER model PR-23R /80710-34) operates between (0 to 1 bar and 4 to 20 Ma) was used. It was fixed at inlet and outlet of hot and cold fluid by mechanical fitting .The configurations of (DPHE) were designed to counter flow path that is the flow direction of the two fluids. The

time needed to achieve the steady state of the working fluids is 1 hour, and the final temperature measured of hot and cold liquids for further measurements of the (U) were stated. The method of (LMTD) is used to determine the (U) inside and outside. All the pipes used to connect part of the system which is (pvc).

Uncertainty Analysis

From Holman and Gajda (1984) the Mean (\bar{x})

$$\bar{X}_{mean} = x_{average} = ((\sum_1^n X_i) / n) \quad (6)$$

Where: (x_i) is the values of each measurement, n: is the total number of measurements of x.

The Standard Deviation (σ): The standard deviation of (x) denoted by (σ), given by.

$$\sigma = \sqrt{\frac{\sum_1^n (x_i - \bar{x})^2}{n - 1}} \quad (7)$$

The standard error or the error in the mean (σ_m): The standard deviation of the mean. It is also called the standard error is denoted by (σ_m) given by:

$$\sigma_m = \frac{\sigma}{\sqrt{n}} \quad (8)$$

The true measured value of (x) given by:

$$x = \bar{x} + \sigma_m = \bar{x} \pm \frac{\sigma}{\sqrt{n}} \quad (9)$$

The calculated uncertainties for the measured parameters are shown in the table (5), the measured parameters included are (heat dissipation rated, Nussle's number, overall heat transfer coefficient and air side Reynold's number, overall heat transfer coefficient.....etc.).

Calibration of Measurement Devices

Temperature Reading

The calibration of 12 thermocouples temperature reading via a calibration device (PROVA MODEL 123) is illustrated in figure (5). The chromium aluminum thermocouple (type K) used in the measurement of temperature is ranged from (-50 °C to 1000 °C). The device calibration signal specified via batteries, and the device converts the signal into a reading of temperature. After that, the device calibration signal transfers to thermometer via a wire of thermocouple. Table (6) shows the device recorded reading. The following points summarize the calibration steps of the apparatus.

- 1- Switch the power on for around 1 minute, so far the symbol disappears.
- 2- Connect the corresponding connectors K type the thermocouple connector with the terminals of the calibration device in order to be calibrated. The sliding switch should be moved to C, F position.
- 3- Press on the keypad (even the minus-button) in order to directly enter the value of temperature.
- 4- Enter the value of temperature from (5 to 95) °C as depicted in figure (6), which presents the schematic diagram to the calibration process.
- 5- The relation between the temperature readings of the two devices is shown in Figure (7). A polynomial equation is derived for correcting the measured temperature readings:

$$T_{calib} = - 0.745 + 1.0294T_{re} + 0.0001 T_{re}^2 - 0.000004 T_{re}^3 \quad (10)$$

Where T_{calib} , is calibrated temperature value, T_{re} is the temperature of measurement by temperature recorder.

Pressure Measuring System Calibration

Pressure transducer set-up was calibrated by connect U-tube manometer is used to measure the pressure difference along the inner tube, At the same time, the port P1 was fixed at the tube inlet of the tube and also port P2 at the exit, measuring the difference pressure between two points with difference values of flow rate. Figure (8) represents the calibration data for pressure taking from transducer and manometer at the same condition. Relation between manometer reading and that measured by pressure sensor was a polynomial equation used to correct the pressure sensor reading.

$$P_{\text{Calib}} = 0.239286 + 0.38593P_{\text{re}} - 0.298269P_{\text{re}}^2 - 0.04243P_{\text{re}}^3 \quad (11)$$

Where P_{calib} is calibrated pressure value, while P_{re} is the pressure measurement by pressure sensor.

Liquid Flow Meter Calibration

The calibrations of flow meters are done using a scaled tank by volume and a stop watch to measure the time required to fill a specified volume of the tank. The calibrations are taken using distilled water the result was tabulated as table (7). The results are very close, see figure (9).

$$Q_{\text{Calibration}} = 0.0556 Q_{\text{re}}^3 - 1.1795 Q_{\text{re}}^2 + 9.2178 Q_{\text{re}} - 18.743 \quad (12)$$

Where (Q_{calib}) is calibrated discharge value, while (Q_{re}) is the flow meter measurement.

Gas Flow meter Calibration

Orifice meters are type of differential meters, all of which infer the rate of gas flow by measuring the pressure difference across a deliberately designed and installed flow disturbance. A standard designed orifice is used to calibrate the gas flow meter since it is easy to field-service and have no moving parts. An orifice meter is a conduit and a restriction to create a pressure drop. It consists of a straight length pipe of 50cm; inside it a central orifice of 14 mm inlet diameter and 45mm outlet diameter is located; which creates a pressure drop, thereby affecting the flow. The pressure deference entered in an equation to compute the air flow rate and compared it with the one measured by the flow meter Holman and Gajda (1984).

$$\dot{V}_{\text{theory}} = V_2 A_2 = \frac{A_2}{\sqrt{1 - \left(\frac{A_2}{A_1}\right)^2}} \sqrt{\frac{2(\Delta P)G}{\rho G}} \quad (13)$$

The computed error is $\pm 6\%$ which is giving the following gas flow meter calibration equation:

$$\dot{V}_{\text{flowmeter}} = 0.96 \dot{V}_{\text{orifice}} \quad (14)$$

Relation between orifice meter reading and that measured by gas flow meter was a polynomial equation used to correct the flowrate readings. as shown in figure (10).

$$\dot{V}_{\text{calib}} = 49.416 + 3.0299 \dot{V}_{\text{re}} + 0.1079 \dot{V}_{\text{re}}^2 + 0.0009 \dot{V}_{\text{re}}^3 \quad (15)$$

Experimental Calculation

Overall heat transfer coefficient (U)

1. Transfer of heat from hot to cold water

$$Q_h = \dot{m}_h \times C_{p,h} \times (T_{h,in} - T_{h,out}) \quad (16)$$

2. Transfer of heat from Cold to Hot Water

$$Q_C = \dot{m}_C \times C_{p,c} \times (T_{c,out} - T_{c,in}) \quad (17)$$

3. Average Heat Transfer

$$Q_{ave} = \frac{Q_c + Q_h}{2} \quad (18)$$

4. (LMTD) Logarithmic mean temperature difference
For counter arrangement of flow

$$LMTD_{CF} = \frac{\Delta T_1 - \Delta T_2}{\ln[\Delta T_1 / \Delta T_2]} \quad (19)$$

$$\text{Where: } \Delta T_1 = T_{h,in} - T_{c,out}; \quad \Delta T_2 = T_{h,out} - T_{c,in}$$

5. The coefficient for total heat transfer (outer pipe)

$$U_o = \frac{Q_{ave}}{A_o LMTD} \quad (20)$$

6. The coefficient for total heat transfer (inner pipe)

$$U_i = \frac{Q_{ave}}{A_i LMTD} \quad (21)$$

The following equation is used without taking into account the word fouling factor for (DPHE):

$$\frac{1}{U_i A_i} = \left[\frac{1}{h_o A_o} \right] + \left[\frac{\ln\left(\frac{D_o}{D_i}\right)}{2 \pi k L} \right] + \left[\frac{1}{h_i A_i} \right] \quad (22)$$

Where U_o , U_i is the outer pipe and inner pipe overall heat transfer coefficient, K is the tube material's thermal conductivity and L is the heat exchanger's length.

Based on the Gnielinski (1976), the outer pipe (HTC) (h_o) is computed and the expression is provided below:

$$Nu_o = \frac{\left(\frac{f}{2}\right)(Re - 1000) Pr}{1.07 + 12.7 \left(\frac{f}{2}\right)^{0.5} (Pr^{2/3} - 1)} \quad (23)$$

$$f = (1.58 \ln(Re) 3.82)^{-2} \quad 2300 < Re < 10^6, \quad 0.5 < Pr < 2000$$

The value of (Nu) obtained through Equation. (23). the outer pipe (HTC) is calculated using the following expression:

$$h_o = \frac{Nu_o \times k_o}{D_h} \quad (24)$$

Where D_h the hydraulic diameter and k_o is the outer pipe's thermal conductivity.

$$D_h = \frac{4A}{p} = (D_o - D_i)$$

The h_o value from equation. (24) Is used in equation (22) for determining the inner pipe (HTC), h_i in the equation, this is the only unknown value. It is possible to calculate the value of Nu_i from:

$$Nu_i = \frac{h_i \times D_i}{k_i} \quad (25)$$

(Re) is depending on the volume flowrate at the inner pipes.

$$Re_i = \frac{\rho_i v D_i}{\mu_i} \quad (26)$$

The (Pr) Prandtl number is computed at mean fluid temperature is calculated using the following expression:

$$Pr_i = \frac{cp_i \mu_i}{k_i} \quad (27)$$

The friction factor of the study is determined due to the change in pressure between the inlet and outlet of the inner pipe, and the formula is given down:

$$f = \frac{\Delta P}{\frac{L_i}{D_i} \times \left(\frac{v^2 \rho_i}{2} \right)} \quad (28)$$

Where: ΔP (pressure drop) = $P_1 - P_2$

Effectiveness – NTU Method

1. NTU :

$$NTU = \frac{U \times A}{C_{min}} \Rightarrow NTU = \frac{Q}{(\Delta T)_{LMTD} \times C_{min}} \quad (29)$$

2. Inner pipe (tube side) fluid's heat capacity

$$C_h = \dot{m}_h \times C_{p,h} \quad (30)$$

3. Outer pipe (annulus side) fluid's heat capacity

$$C_c = \dot{m}_c \times C_{p,c} \quad (31)$$

4. The effectiveness of (DPHE)

$$\varepsilon = \frac{1 - \exp[-NTU(1-N)]}{1 - N \exp[-NTU(1-N)]} \quad (32)$$

Where: $N = \frac{C_{min}}{C_{max}}$

Thermo-Physical Properties of Two-Phase (air –water)

$$V = \frac{\dot{V}_a + \dot{V}_f}{\frac{\pi}{4} D_i^2} \quad (33)$$

$$\rho = \frac{\rho_a \dot{V}_a + \rho_f \dot{V}_f}{\dot{V}_a + \dot{V}_f} \quad (34)$$

$$\mu = \frac{\mu_a \dot{V}_a + \mu_f \dot{V}_f}{\dot{V}_a + \dot{V}_f} \quad (35)$$

$$Vf = \frac{\dot{V}_a}{\dot{V}_a + \dot{V}_f} \quad (36)$$

Where **Vf** is the Void fraction and the range is between (0.1 – 0.9).

The Exergy Loss Analysis

In general, Exergy (E) is described as the maximum useful work that can be obtained in a specified environment from the reversible system.

In current study, the inquiry into the Exergy is based on irreversibility of heat transfer. Dimensionless Exergy loss (e) was measured using a model of study Yildiz and Pehlivan (1997), as stated below. Exergy balance can be defined as:

$$\sum E_{in} = \sum E_{out} - \sum E_{Product} \quad (37)$$

The (HE) was adiabatic in this experiment and the value of (Q_{co}) was believed to be equal to the amount (Q_{ho}). The Exergy loss in a steady-state control volume and the expression is provided below:

$$E = E_h + E_{co} \quad (38)$$

E_h and E_{co} are the exergy change for hot water and cold water respectively and are calculated as follows:

$$E_h = T_e [m_h (S_{h,out} - S_{h,in})] \quad (39)$$

$$E_c = T_e [m_{co} (S_{co,out} - S_{co,in})] \quad (40)$$

The change in entropy can be measure as :

$$S_{out} - S_{in} = C_{p,co} \ln\left(\frac{T_{out}}{T_{in}}\right) \quad (41)$$

Substituting Eq. (41) into Eq. (38), (39) and (40) yields.

$$E_h = T_e \{ m_h C_{p,co} \ln\left(\frac{T_{out}}{T_{in}}\right) \} \quad (42)$$

$$E_c = T_e \{ m_c C_{p,co} \ln\left(\frac{T_{out}}{T_{in}}\right) \} \quad (43)$$

$$E = T_e \left\{ \dot{m}_h C_h \ln\left(\frac{T_{h,out}}{T_{h,in}}\right) + \dot{m}_{co} C_{co} \ln\left(\frac{T_{co,out}}{T_{in,in}}\right) \right\} \quad (44)$$

Finally, the (e) dimensionless Exergy loss is calculated as below:

$$e = [E / (T_e * C_{min})] \quad (45)$$

RESULTS AND DISCATION

Steps of Les Engine Model

The measured temperature, pressure and flow rates allowed calculating the heat transfer rates, friction factor, effectiveness, specific exergy, NTU, Overall heat transfer and inner Nusselt number from the tube side of double - pipe heat exchanger for turbulent flow. The effect of injection air bubbles at different volume flowrate of air (12, 16 and 20 l/min) variation with volume flow rate inside annulus side (8, 10, 12 and 14 l/min) at one volumes flow rate of tube side (8 l/min) at different volume concentration of Al₂O₃ nanofluid on heat transfer and friction factor are studied. Therefore, in the present part, experimental results have been presented and discussed.

Case of Distilled Water

The primary test has been done with warm water running inside the inner pipe when the cold water was flowing through the outer pipe. This is to assess the precision of the comparison calculation when using nanofluids instead of water. Fig. 11 indicates the comparing for both the established correlation Indicated by **Gnielinski** and experimental result. The average deviation observed is ± 6 %, within reasonable limits, suggesting that the methods used to calculate experimental data could be used for estimate nanofluid (HTC). This means the experimental system is calibrated and able to work the experiments with variable air bubble injection and nanofluid concentration.

Nusselt Number of Double Pipe Heat Exchanger (tube- side)

Figure (12) it is clear that the Nusselt number for nanofluid is more than the base fluid because of increasing thermal conductivity and the Brownian motion of nanoparticles. The increasing in volume concentration leads to increase in thermal conductivity and viscosity but decreases in specific heat.

The variation of Nusselt number with volume flow rate of water in annulus side vary from (8, 10, 12 and 14 l/min), and at 8 l/min of hot fluid in tube side, for single phase and two - phase flow with air bubbles injection has volume flow rate range (12, 16 and 20 l/min) in counter flow direction under turbulent condition. It can be observed the Nusselt number increase with increasing volume flow rate of cold water for all value of air flow rate This is due to increasing Nusselt number and for the same reason the air increases turbulence and mixing in annulus side so that two phase flow increase Nusselt number. For pure water (single phase), Nusselt number increase from (40.46) at 8 l/min to (50.79) 14 l/min but for two phase flow at volume flow rate for air is 20 l/min the Nusselt number increase with cold water flow rate from (68.37) at 8 l/min to (118.9) at 14 l/min. Figure (13) shows the Nusselt number change with water flow rate in annulus side for various Al_2O_3 nanofluid concentration (0.1, 0.2 and 0.3 % by volume) in counter flow direction. It's shown the nanoparticle enhancement the Nusselt number of heat exchanger at 14 l/min annulus side volume flow rate, and at volume flow rate for air is 12 l/min the Nusselt number enhance from (86.12) to (89.69) after addition 0.3 % Al_2O_3 nanoparticle. Nusselt number increase with increasing nanoparticle concentration. This is due to higher inner heat transfer coefficient and thermal conductivity.

Number of Thermal Unit (NTU) of Double Pipe Heat Exchanger

Figures (14) include the variation between NTU of double pipe heat exchanger with volume flow rate in annulus side, for single phase and two-phase flow with air bubbles injection has volume flow rate range (12 , 16 and 20 l/min) in counter flow direction under turbulent condition. It can be observed the NTU increase with increasing flow rate in annulus side when the volume flow rate in hot fluid in tube side is 8 l/min. Minimum thermal capacity (C_{min}) for hot fluid and it is constant at 8 l/min. It has been seen according to equation (18) increase cold water volume flow rate in annulus side will be increase. For pure water (single phase), NTU increase from (0.3863) at 8 l/min to (0.5047) 14 l/min but for two phase flow at volume flow rate for air is 20 l/min the NTU increase with cold water flow rate from 0.693 at 8 l/min to 0.9898 at 14 l/min. The thermal boundary layer that is created on the outer surface of the tube side has been shown to be mixed, and when the air bubble injection increase turbulence and mixing. Figure (15) exposes effect the Number of thermal unit (NTU) with the volume flowrate of water in outer tube for different Al_2O_3 nanofluid concentration (0.1, 0.2 and 0.3 % by volume). It can be observed the adding nanoparticle to water which enhancement the NTU of heat exchanger at 14 l/min annulus side volume flow rate, and at volume flow rate for air is 12 l/min the NTU enhance from 0.8237 to 0.9682 after addition 0.3 % Al_2O_3 nanoparticle. NTU increase while increase nanoparticle concentration. This due to increase thermal conductivity by reduce temperature different between wall and bulk temperature that increase overall heat transfer coefficient depend on equation (29).

Specific Exergy of Double Pipe Heat Exchange

Figure (16) show that the exergy losses (E) increase with increased volume flow rate of water in annulus side. To this reason, dimensionless exergy loss (e) increase with annulus side flow rate depend on equation (44). The air bubble motion will raise the turbulence rate of the outer pipe and mix the thermal boundary layer formed on the outer surface of the inner pipe . In Addition, the volume fraction is decreased by pumping of the air bubbles within the (HE). For single phase (pure water) the specific exergy slightly increase from 0.1088 at 8 l/min to 0.1704 at 14 l/min but for two phase flow at volume flow rate for air is 20 l/min. Figure (17) indicates the specific exergy variation with water volume flow rate in annulus side for

different Al₂O₃ nanofluid concentration (0.1, 0.2 and 0.3 % by volume). It can be observed the adding nanoparticle to water which enhancement the specific exergy of (HE) at 14 l/min annulus side flow rates, and at volume flow rate for air is 12 l/min the specific exergy enhances from 0.2659 to 0.2818 after addition 0.3 % Al₂O₃ nanoparticle. Specific exergy increases while increase nanoparticle concentration. This increment due to increasing of thermal conductivity for nanofluid and decreasing the thickness of thermal boundary layer then temperature difference decreases so the exergy loss rate increases according to equation (44).

CONCLUSIONS

The current study focused mainly on calculating the performance of the (DPHE) under turbulent flow conditions with (U bend) for counter flow arrangement. The performance of the (HE) is evaluated in expression of (NTU) and (E). The (NTU) procedure contains both the cold and hot fluid flowrates. Two heat transfer enhancement techniques (1) active technique and (2) passive technique were included in this study. Add Al₂O₃ Nanofluid and bend in the test tube at a distance of 2 m to achieve the active technique of heat transfer increase. To achieve the passive technique of heat transfer enhancement, air bubble injection were used. The following some important conclusions from the study are provided below:

1. The experimental results indicate that Number of thermal unit (NTU) was increased by increasing particles volume concentrations and volume flow rate have been observed.
2. Air bubble injection is one of the promising and inexpensive techniques that can reasonably enhance the thermal increase in the heat transfer coefficient and Nusselt Number with increase in the air volume flow rate have been observed. The high rate of bubbles injection had more effect on heat transfer enhancement.
3. Depending on pumping case and outer pipe volume flowrate (cold water) an increase in NTU up to (1.5 – 4.2) times, (1.23 – 2.59) times in (e) and (1.36 – 2.44) in (ε) comparing to the base fluid (pure water) without injection of air bubble were obtained.
4. Adding nanoparticles to the base fluids increases the efficiency of the heat exchanger, but there is also a loss in the pumping capacity. The penalty of friction is negligible when compared to heat transfer improvements.
5. Number of transfer unit increased 1,041 times and effectiveness 1,021 times at volume flow rate of 14 l / min for 0.3 % nanofluid. Also the efficiency for the heat exchanger is improved 1.008-times at a concentration of 0.3 % volume with a volume flowrate 14 l/min.

Table (1): Al₂O₃ Nanoparticles and base fluid characteristics.

	ρ (kg/m ³)	C _p (J/kg °C)	k (W/m.°C)	μ (kg/m.s) x 10 ⁻³
Al ₂ O ₃	3970	765	40	-
Pure water at 60 °C	983.3	4179	0.595	0.949

Table (2): Computation of nanofluid properties at 60 °C.

φ	k _{nf} (W/m. °C)	μ _{nf} (kg/m.s)	C _p _{nf} (J/kg °C)	ρ _{nf} (kg/m ³)
0.1	0.617	0.00102	4046.97	1027
0.2	0.635	0.00113	3922.47	1057
0.3	0.653	0.00162	3804.87	1087

Table (3): Specifications of Ultrasonic Cleaner Bath

Model	JTS-1018
Tanks working dimension (mm)	L ₁ = 406 , W ₁ =305, H ₁ =460
Overall dimension (mm)	L ₁ = 586 , W ₁ =485, H ₁ =680
Ultrasonic frequency	40 kHz
Ultrasonic power	720 Watt (variable)
Digital timer control	1-30 min
Capacity	54 liter
Temperature control range (°C)	< 90 °C
Ultrasonic power output	800 W

Table (4): Mass of each concentration add to five liter of distilled water.

φ%	0.1%	0.2%	0.3%
Mass (gram)	19.2	38.4	57.6

Table (5): Measurements Uncertainties.

variable	Reading of parameter			x _m	σ	σ _m	x	Percentage Uncertainty
	x ₁	x ₂	x ₃					
T _{outlet tube}	45.90	45.10	44.70	45.23	0.61	0.35	45.59 44.88	± 0.78 %
T _{outlet annulus}	38.20	39.28	38.45	38.64	0.57	0.33	38.97 38.32	± 0.84 %
Re _h	0.0173	0.0168	0.0167	0.017	0.0003	0.0002	0.017192 0.016828	± 1.07 %
Re _{co}	0.018	0.0172	0.0177	0.018	0.0004	0.0002	0.0179 0.0174	± 1.35 %
Q _{ave}	1111	1079	1119	1103	21.17	12.22	1115.22 1090.78	± 1.11 %
Nu	71.04	40.17	63.74	58.32	16.13	9.31	67.63 49.00	± 15.97 %
h	4227	3390	3793	3803.3	418.6	241.68	4045.01 3561.66	± 6.35 %
U _{in}	243.7	256.5	255.5	251.9	7.12	4.11	256.01 247.79	± 1.63 %
U _o	203.1	213.7	212.9	209.9	5.90	3.41	213.31 206.49	± 1.62 %
ε	0.4054	0.4235	0.4282	0.42	0.01	0.01	0.43 0.41	± 1.66 %
NTU	0.6735	0.7295	0.734	0.71	0.03	0.02	0.73 0.69	± 2.73 %
LMTD	22.72	20.97	21.82	21.84	0.88	0.51	22.34 21.33	± 2.31 %
e	0.2248	0.2089	0.2121	0.22	0.01	0.00	0.22 0.21	± 2.26 %

Table (6): Reading of Calibration Process of Temperature Recorder

T (°C) in calibrated device of standard wire	T (°C) in temperature recorder of standard wire
5	4.5
16	15.5
28	28.1
34	34.4
50	50.3
60	60.6
80	80.1
95	94.5

Table (7): Reading of Calibration Process of flowrate Recorder

Stander volume flowrate (l/min)	Actual volume flowrate (l/min)
6	6.09
6.5	6.6
7	7.09
7.5	7.44
8	7.88
8.5	8.61
9	9.14



Fig. (1) Ultrasonic Cleaner

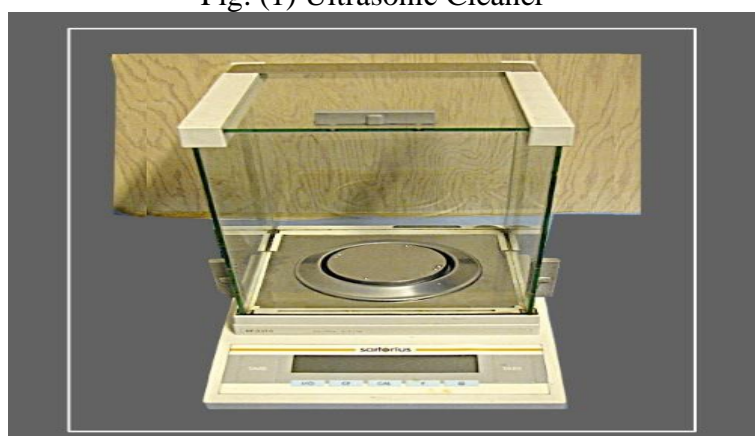


Fig.(2) Electronic Weighting Machine

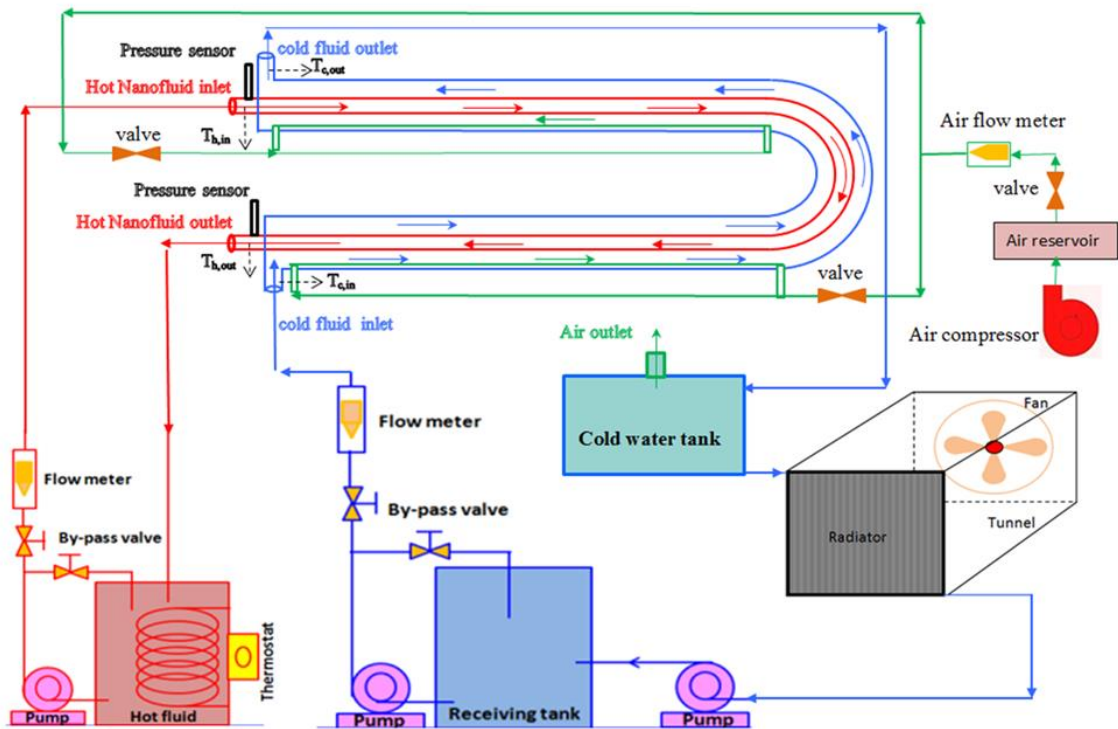


Fig. (3): Schematic diagram of experimental setup

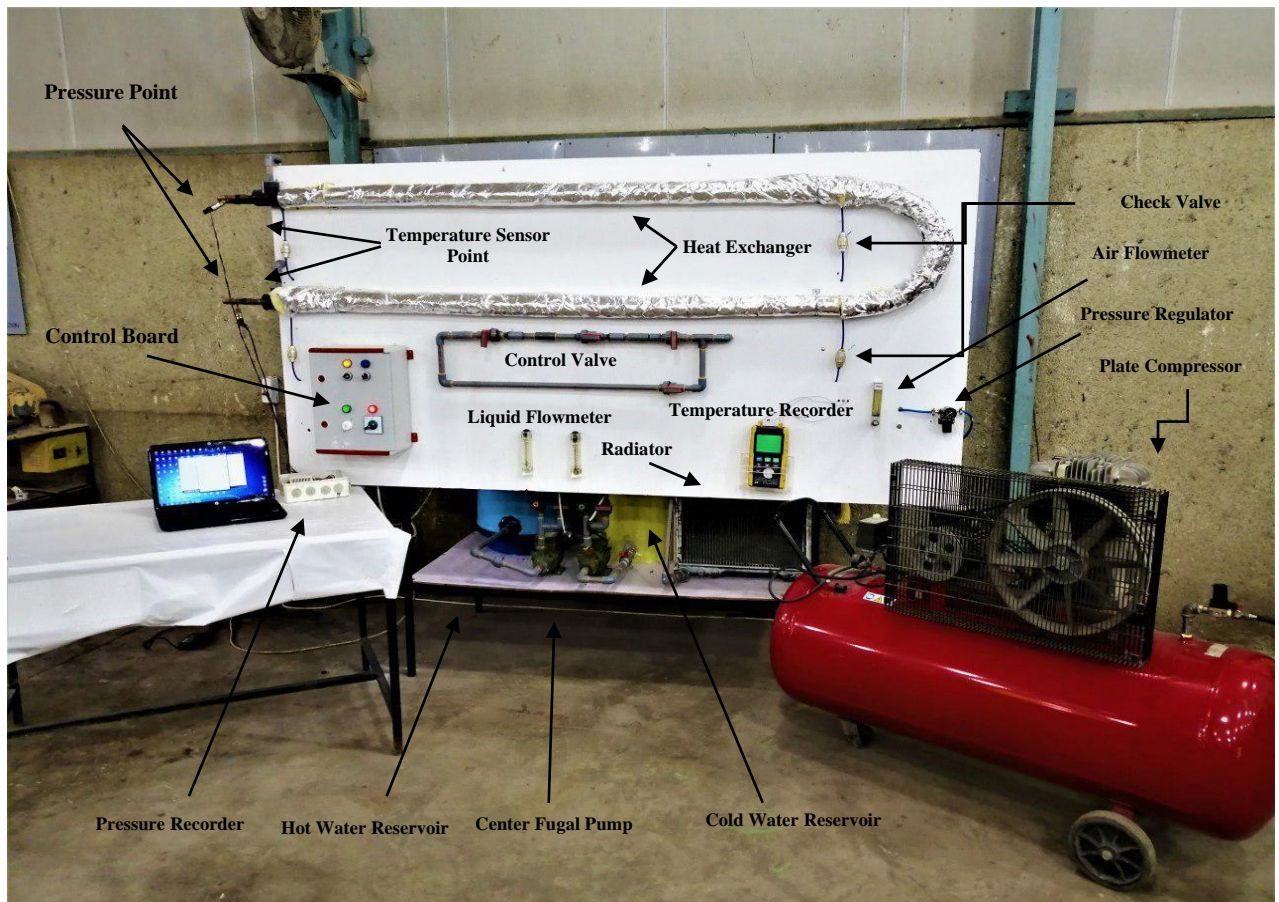


Fig.(4): Photographic presentation of experimental setup

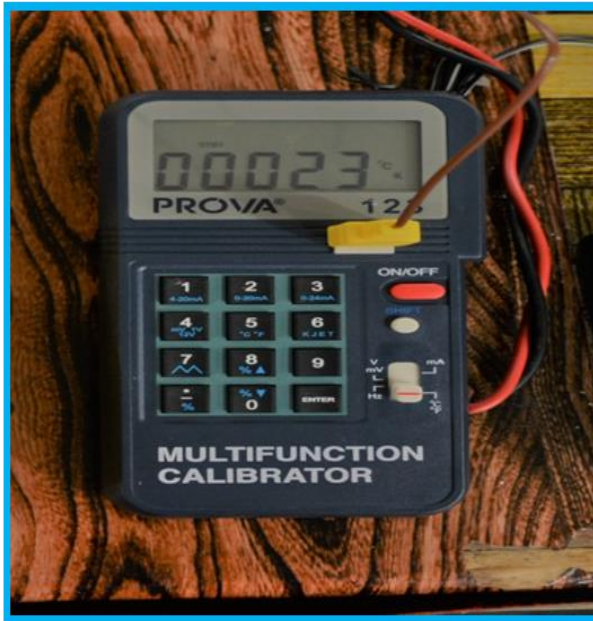


Fig. (5) Calibration Device (PROVA MODEL 123)



Fig. (6) Photograph of Temperature Data Logger with Calibration Device

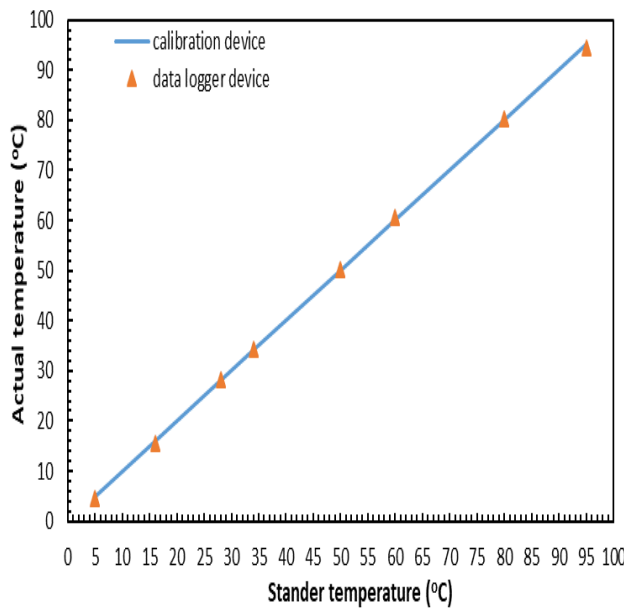


Fig. (7): Calibration Curve of Temperature Recorder Readings

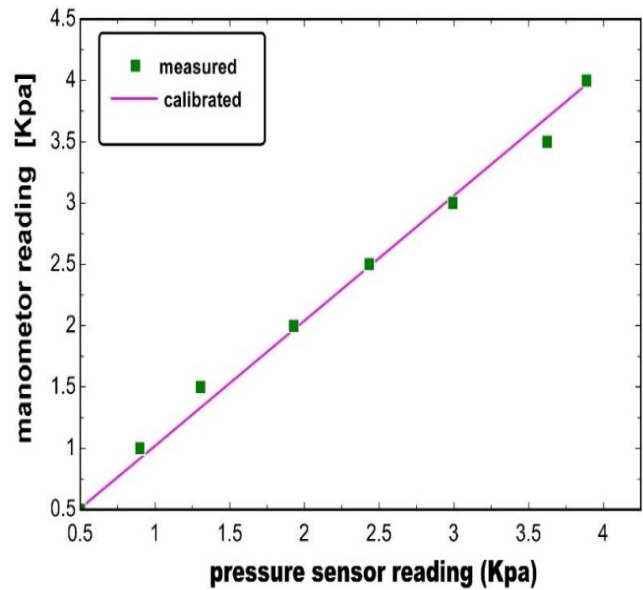


Fig. (8) Calibration Curve of Pressure Sensor.

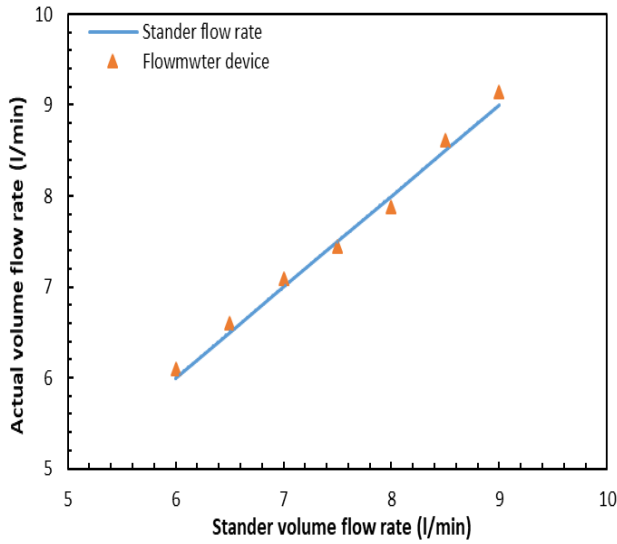


Fig. (9) Flow Meter Accuracy Reading

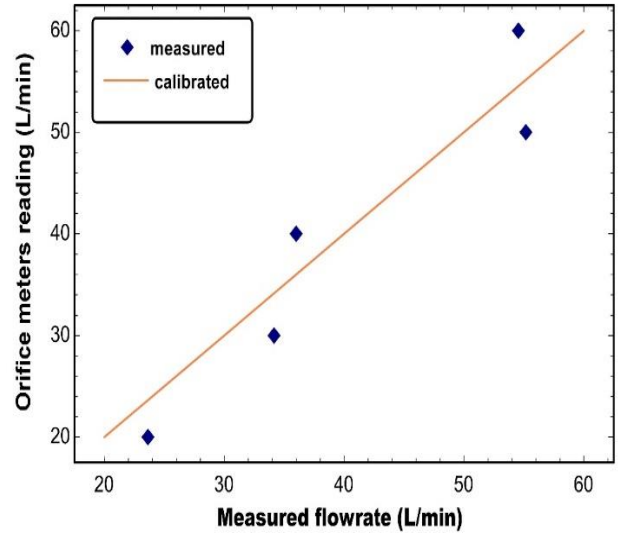


Fig. (10) Calibration of the Gas Flow Meter.

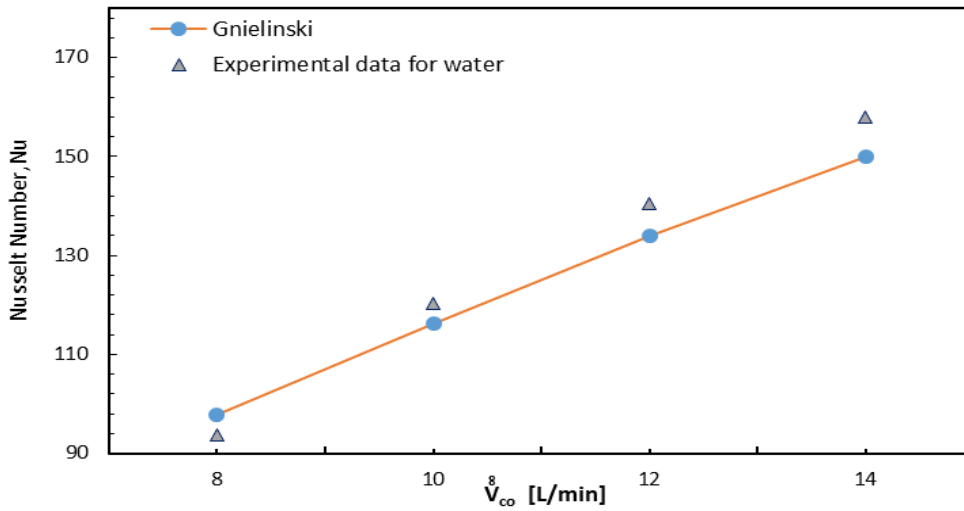
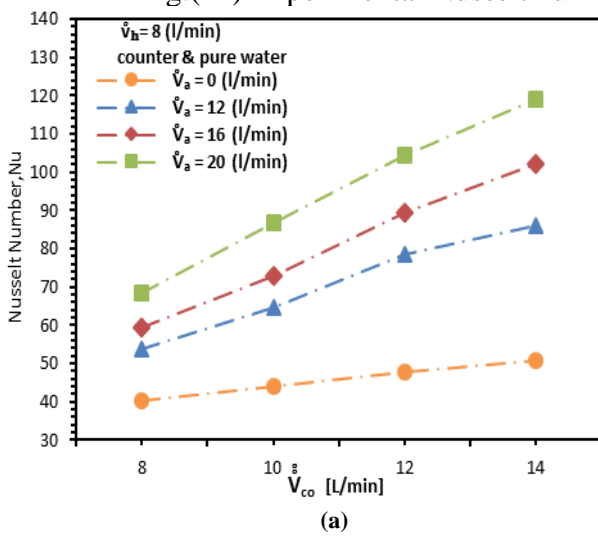
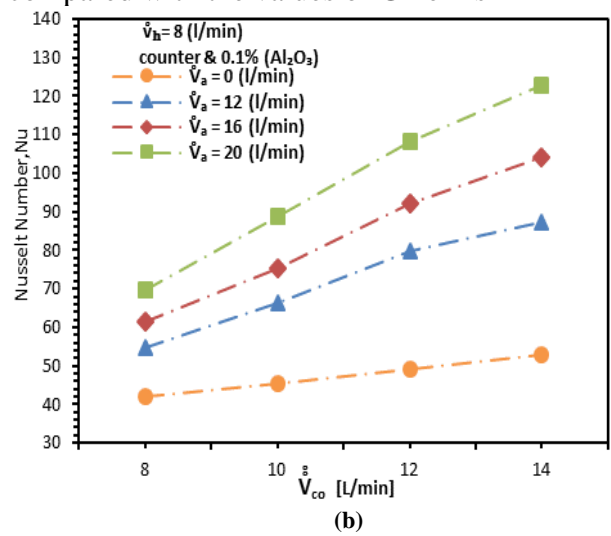


Fig.(11) Experimental Nusselt number is compared with the values of Gnielinski



(a)



(b)

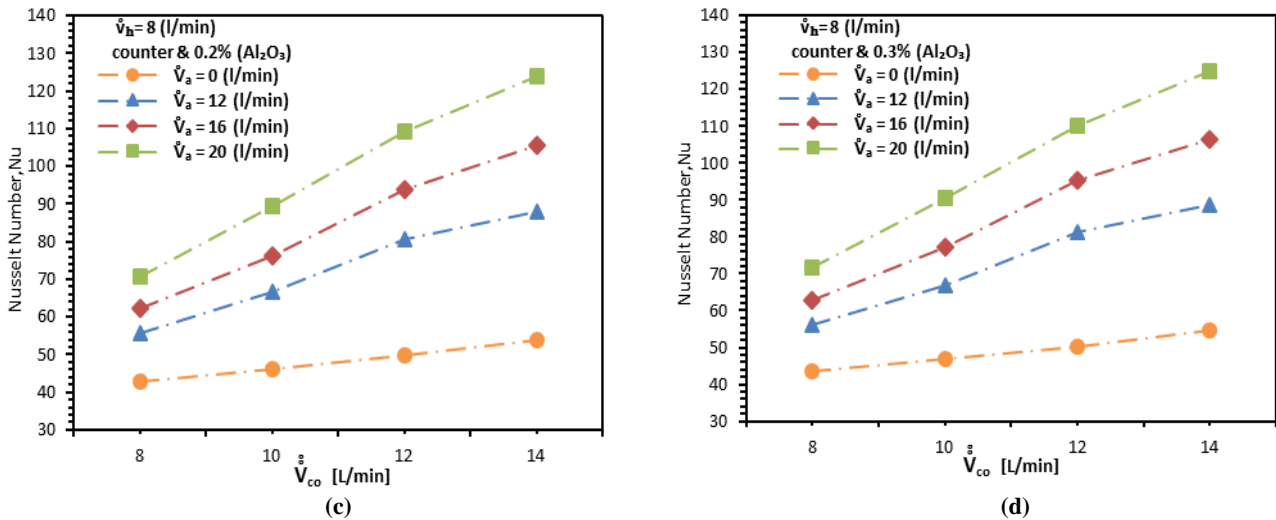


Fig. (12) variation of Nusselt number with volume flowrate of cold water at (8 l/min) of nanofluid (CF) (a) pure water , (b) 0.1 % of Al₂O₃ , (c) 0.2 % of Al₂O₃ and (d) 0.3 % of Al₂O₃

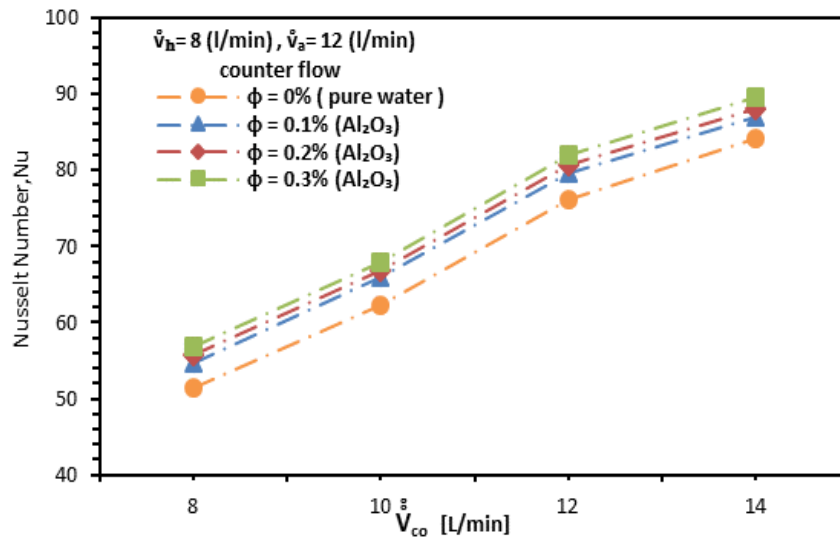
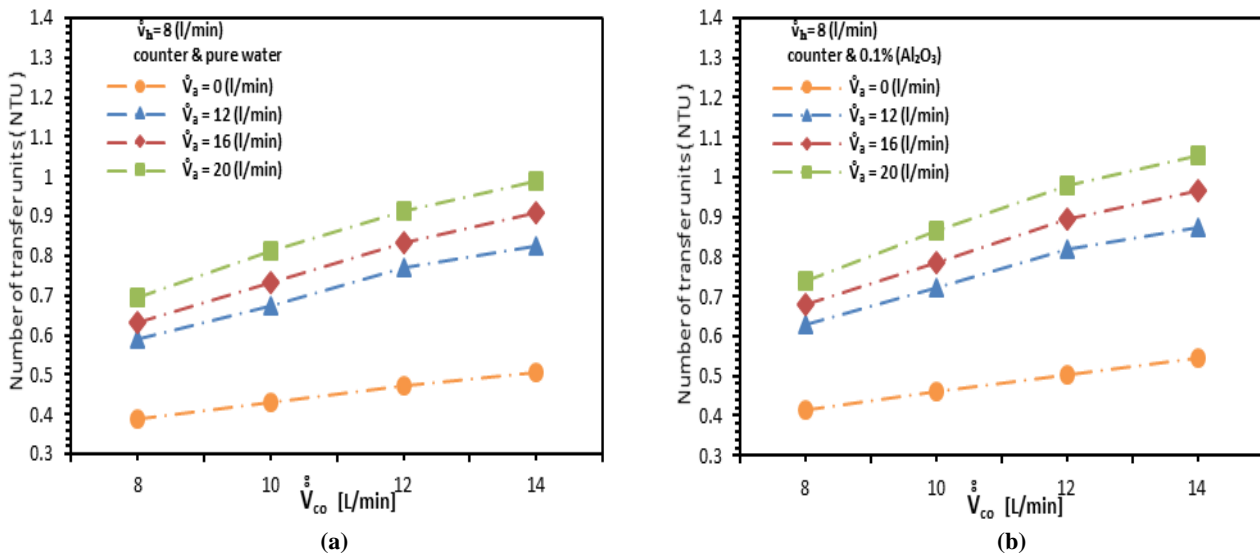


Fig. (13) Variation of Nusselt number with volume flowrate of cold water at (8 l/min) and volume concentrations



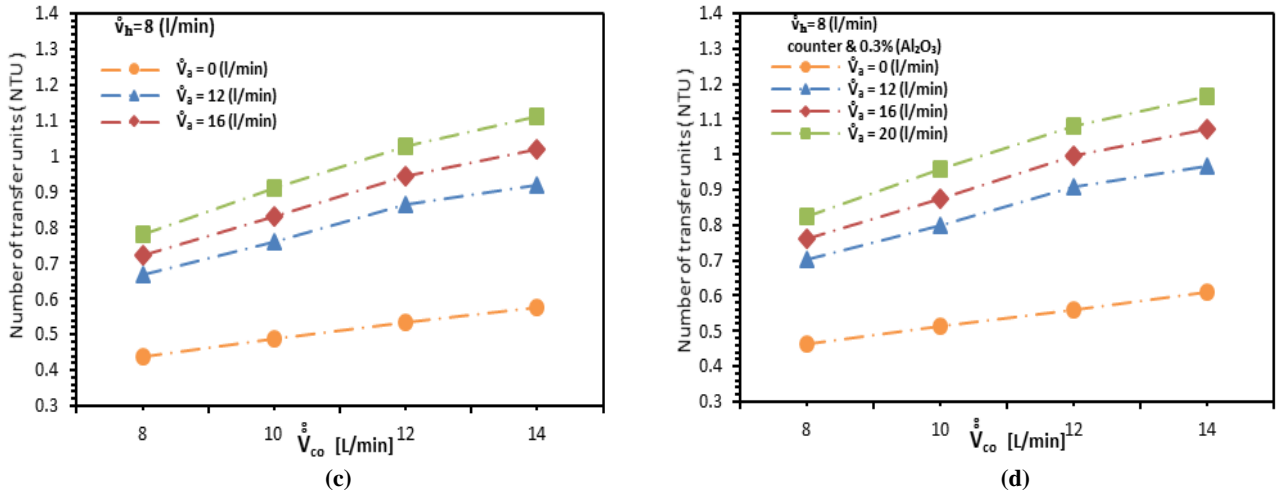


Fig. (14) variation of NTU with volume flowrate of cold water at (8 l/min) of nanofluid (CF) (a) pure water , (b) 0.1 % of Al_2O_3 , (c) 0.2 % of Al_2O_3 and (d) 0.3 % of Al_2O_3

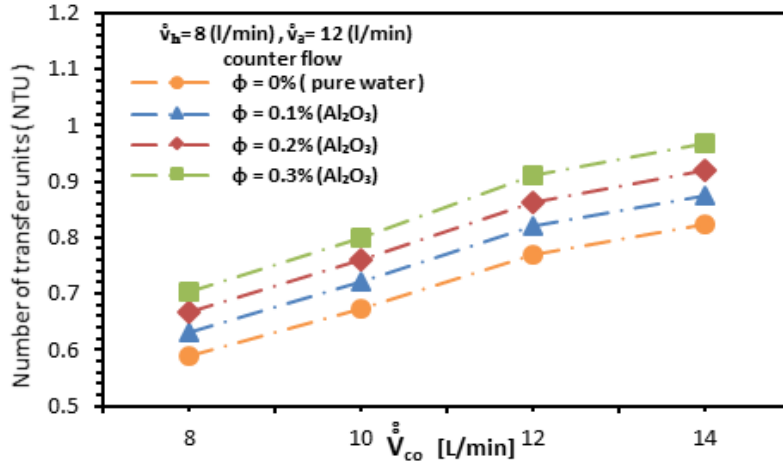
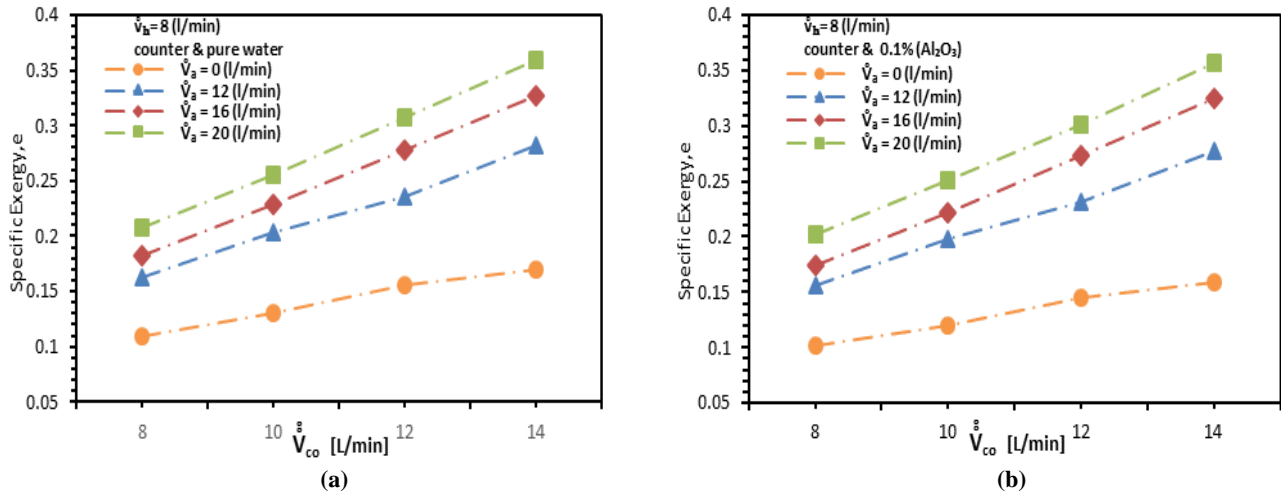


Fig. (15) Variation of NTU with volume flowrate of cold water at (8 l/min) and volume concentrations



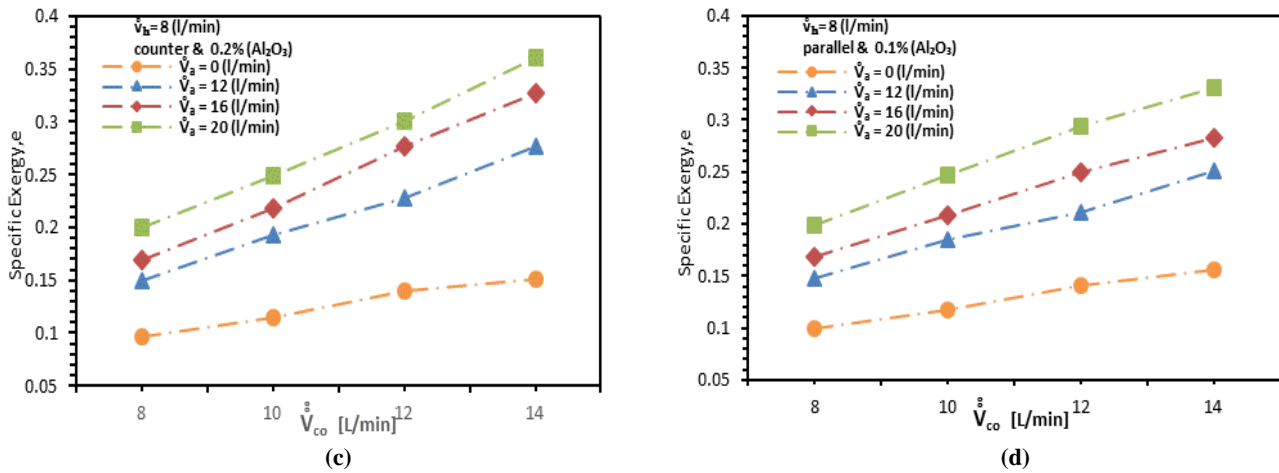


Fig. (16) variation of specific exergy with volume flowrate of cold water at (8 l/min) of nanofluid (CF) (a) pure water , (b) 0.1 % of Al_2O_3 , (c) 0.2 % of Al_2O_3 and (d) 0.3 % of Al_2O_3

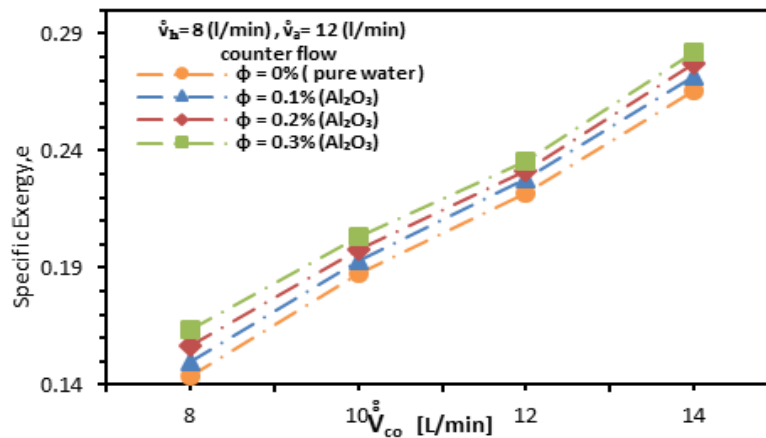


Fig.(17): Variation of specific exergy with volume flowrate of cold water at (8 l/min) and volume concentrations

REFERENCES

- Kahrom, Mohsen, Payam Haghparast, and S. M. Javadi, "Optimization of heat transfer enhancement of flat plate based on pereto genetic algorithm", International Journal of Engineering, Transaction A: Basics, Vol. 23, No. 2, 177-190, 2010.
- A. Kitagawa, K. Kitada, and Y. Hagiwara, "Experimental study on turbulent natural convection heat transfer in water with sub-millimeter-bubble injection," Experiments in fluids, Vol. 49, No. 3, pp. 613-622, 2010.
- H. S. Dizaji and S. Jafarmadar, "Heat transfer enhancement due to air bubble injection into a horizontal double pipe heat exchanger " International Journal of Automotive Engineering Vol. 4, No. 4, pp. 902-910, 2014.
- H. S. Dizaji, S. Jafarmadar, M. Abbasalizadeh, and S. Khorasani, "Experiments on air bubbles injection into a vertical shell and coiled tube heat exchanger; exergy and NTU analysis," Energy Convers. Manag., Vol. 103, pp. 973–980, 2015.

G. SINGH and A. NANDAN, "Experimental study of heat transfer rate in a shell and tube heat exchanger with air bubble injection," *International Journal of Engineering*, Vol. 29, No. 8, pp. 1160-1166, 2016.

Mohammad Mahdi Heyhat, Adel Abdi and Ali Jafarzad, Performance Evaluation and Exergy Analysis of a Double Pipe Heat Exchanger under Air Bubble Injection, *Applied Thermal Engineering*, Vol. 143, pp. 582-593, 2018.

J. Albadr, S. Tayal, and M. Alasadi, "Heat transfer through heat exchanger using Al₂O₃ nanofluid at different concentrations," *Case Stud. Therm. Eng.*, Vol. 1, No. 1, pp. 38-44, 2013.

D. Han, W. He, and F. Asif, "Experimental study of heat transfer enhancement using nanofluid in double tube heat exchanger," *Energy Procedia*, vol. 142, pp. 2547-2553, 2017.

M. B. P. Rao, M. V. N. Rao, S. R. M. Naidu, and M. T. Veeraiah, "Heat Transfer Enhancement in Double Pipe Heat Exchanger by Alumina–Water Nanofluid," *Heat Transfer*, Vol. 5, 2018.

S. Lee, S.-S. Choi, S. Li, and J. A. Eastman, "Measuring thermal conductivity of fluids containing oxide nanoparticles," *J. Heat Transfer*, Vol. 121, No. 2, pp. 280-289, 1999.

B. C. Pak and Y. I. Cho, "Hydrodynamic and heat transfer study of dispersed fluids with submicron metallic oxide particles," *Experimental Heat Transfer an International Journal*, Vol. 11, No. 2, pp. 151-170, 1998.

H. Brinkman, "The viscosity of concentrated suspensions and solutions," *The Journal of Chemical Physics*, Vol. 20, No. 4, pp. 571-571, 1952.

Zan Wu, Lei Wang and Bengt Sundén "Pressure drop and convective heat transfer of water and nanofluids in a double-pipe helical heat exchanger", *Applied Thermal Engineering*, Vol. 60, No. 1-2, pp.266-274 ,2013.

Fotukian S.M., and Nasr Esfahany M., " Experimental investigation of turbulent convective heat transfer of dilute γ -Al₂O₃/water nanofluid inside a circular tube " *International Journal of Heat and Fluid Flow*. Vol. 31, No. 4, pp 606-612., 2010.

J. P. Holman, and Gajda, W.J, *Experimental Methods for Engineers*, Fourth Edition ed.: McGraw-Hill Book Company, 1984.

V. Gnielinski, "New equations for heat and mass transfer in turbulent pipe and channel flow," *Int. Chem. Eng.*, Vol. 16, No. 2, pp. 359-368, 1976.

C. Yildiz, Y. Biçer, and D. Pehlivan, "Heat transfer and pressure drop in a heat exchanger with a helical pipe containing inside springs," *Energy conversion and management*, Vol. 38, No. 6, pp. 619-624, 1997.